Physiological Measurement

Frequency dependent characterisation of impedance changes during epileptiform activity in a rat model of epilepsy

To cite this article before publication: Sana Hannan *et al* 2018 *Physiol. Meas.* in press https://doi.org/10.1088/1361-6579/aad5f4

Frequency dependent characterisation of impedance changes during epileptiform activity in a rat model of epilepsy

Sana Hannan*, Mayo Faulkner, Kirill Aristovich, James Avery, David Holder
Department of Medical Physics and Biomedical Engineering, University College London, UK
Email: sana.hannan.14@ucl.ac.uk*

Abstract

Objective. Electrical Impedance Tomography (EIT) can be used to image impedance changes associated with epileptiform activity and so holds therapeutic potential for improving presurgical localisation of the ictal onset zone in patients with treatment-resistant epilepsy. There are two principal impedance changes which occur during seizures that may be imaged with EIT: (a) a fast, transient impedance decrease over milliseconds due to hypersynchronous neuronal depolarisation in individual ictal discharges; and (b) a larger, slow impedance increase caused by cell swelling over the course of the seizure. The magnitude of these signals is highly dependent on the carrier frequency of applied current used for obtaining impedance measurements. The purpose of this work was to characterise the frequency response of the fast and slow impedance changes during epileptiform activity. *Approach.* Seizures were induced in anaesthetised rats by electrically stimulating the cerebral cortex. During each seizure, impedance measurements were obtained by delivering 50 μA, through two electrodes on an epicortical array, at one of 20 frequencies in the 1-10 kHz range. Recordings were demodulated to determine the magnitude of fast and slow impedance responses at each frequency. *Main results.* The fast impedance change during averaged ictal discharges reached a maximal amplitude and signal-to-noise ratio (SNR) of -0.36 ± 0.05 % and 50.2 ± 11.3, respectively, at 1355 Hz. At this frequency, the slow impedance change had an amplitude of 4.61 ± 1.32 % and an SNR of 545 ± 125, which did not significantly change across frequency ($p > 0.01$). *Significance.* We conclude that the optimal frequency for imaging epileptiform activity is 1355 Hz, which maximises the SNR of fast neural changes whilst enabling simultaneous measurement of slow changes. These findings will inform future investigations aimed at imaging epilepsy in subcortical brain structures, where SNR is considerably reduced, and those using parallel, multi-frequency EIT.

Keywords: electrical impedance tomography, epilepsy, seizure, ictal discharge, cerebral cortex, rat

Submitted to: Physiol. Meas.

1. Introduction

1.1. Background

Electrical Impedance Tomography (EIT) is a medical imaging modality in which the internal electrical impedance of an object is imaged using boundary voltage measurements from peripherally placed electrodes (Holder, 2005a). In conjunction with conventional electroencephalography (EEG) monitoring methods, EIT holds therapeutic potential for improving localisation of the epileptogenic zone in patients with treatment-resistant epilepsy who are candidates for surgery (Boone, et al., 1994; Rao, 2000; Fabrizi, et al., 2006). For this purpose, there are two principal impedance changes which occur during epileptic activity that are suitable targets for imaging: (a) an impedance increase during seizures; and (b) a smaller, transient impedance decrease during individual epileptic discharges.

1.1.1. Impedance changes during epileptiform activity

A well-established increase in cerebral tissue impedance, which occurs over seconds, has been reported in several species during both chemically and electrically induced seizures in acute and chronic models

of epilepsy (Van Harreveld & Schadé, 1962; Elazar, et al., 1966; Rao, 2000; Olsson, et al., 2006; Vongerichten, et al., 2016). It is caused by cell swelling due to a disturbance in ion homeostasis which occurs as a result of the high metabolic demands of the intense neuronal activity underlying epilepsy (Andrew & MacVicar, 1994; Dzhala , et al., 2000; Dreier, et al., 2011). It can also precede the onset of epileptic events by predisposing local neuronal networks to become hypersynchronous, leading to the transition from a pre-seizure to seizure state (Andrew, 1991; Jefferys, 1995; Olsson, et al., 2006; Broberg, et al., 2008). When injected at frequencies below 50 kHz, the majority of current applied to cerebral tissue does not cross the highly-resistive neuronal cell membranes and so is conducted through the extracellular fluid (Seoane, et al., 2005). A decrease in volume of the extracellular fluid due to cell swelling will, therefore, cause an increase in the measured tissue impedance.

The fast impedance changes associated with individual ictal and interictal epileptiform discharges may also be used for localising the seizure onset zone with EIT. These discharges are caused by hypersynchronous depolarisation of local neuronal populations in the brain due to the opening of voltage-dependent sodium and calcium ion channels (Stafstrom, 2007; Cain & Snutch, 2012). As a result, current is able to pass across the cell membrane into activated neurons, leading to a rapid impedance decrease lasting several milliseconds. This phenomenon has been reported in the anaesthetised rat during both interictal and ictal spikes induced by chemical and electrical models of epilepsy, respectively (Vongerichten, et al., 2016; Hannan, et al., 2017).

1.1.2. Frequency dependence of physiological impedance signals

The amplitude of the fast and slow impedance changes associated with epileptic activity is highly dependent on the carrier frequency, the frequency of the sinusoidal current applied to obtain the impedance measurements. Several models have been developed to characterise the frequency dependence of impedance responses during such physiological events.

Liston et al. used a cable theory-based mathematical model to predict the frequency dependence of fast impedance changes during neuronal depolarisation in the unmyelinated axon of a crab peripheral nerve as well as the human cerebral cortex (Liston, et al., 2012). In each case, the predicted impedance change was maximal at DC and decreased rapidly at frequencies above 1 kHz. Recent, more realistic, biophysical modelling of impedance changes in single and multiple unmyelinated nerve fibres, based on the Hodgkin-Huxley model (Hodgkin & Huxley, 1952), has taken into consideration the active sodium and potassium ion channels, in addition to the passive leakage channels, involved in generating action potentials (Tarotin, et al., 2017). This study also showed that the impedance change during depolarisation monotonically decreases with frequency, and can be explained by the capacitive properties of the neuronal membrane (Tarotin, et al., 2017). Contrary to these models, however, experimental findings in the rat cerebral cortex and thalamus demonstrated that the impedance change during somatosensory evoked potentials increased from 1 kHz to 1.5 kHz, and then decreased to a constant minimal value by 3 kHz (Faulkner, et al., 2018). The limitations of the modelling studies, which did not consider the active and passive properties of membranes of interacting myelinated and unmyelinated nerve fibres, may explain this apparent discrepancy (Liston, et al., 2012; Tarotin, et al., 2017). Thus, for epileptic spikes originating in the cerebral cortex or thalamus, the fast impedance change due to the underlying hypersynchronous neuronal firing may be expected to exhibit a frequency response more comparable to that reported during evoked physiological activity (Faulkner, et al., 2018).

Seone et al., predicted the frequency dependence of the slow transencephalic impedance change which occurs during pathological cell swelling in cerebral hypoxia (Seoane, et al., 2005). Using the expression derived by Cole (Cole, 1928), the brain tissue was modelled as a suspension of spherical cells in a conductive fluid (Seoane, et al., 2005). The model tested frequencies in the 20-750 kHz range and predicted a gradual decrease in impedance change with frequency, consistent with experimental data obtained using four epicortical electrodes in anaesthetised piglets (Seoane, et al., 2005). This may be explained by the fact that current applied at higher frequencies (>50 kHz) is able to use intracellular, as

well as extracellular, fluid to traverse neural tissue; since intracellular fluid is more conductive, this results in a decrease in the magnitude of the tissue impedance change with frequency during global cell swelling (Seoane, et al., 2005; Vongerichten, et al., 2016). The behaviour of epileptic tissue during seizures, which are often accompanied by cell swelling, is expected to have similar bioelectrical properties at these frequencies.

1.1.3. Frequencies used for imaging epilepsy with EIT

Since the magnitude of the measured tissue impedance depends on the frequency of applied current, it is necessary to determine the optimal frequency for imaging the fast and slow impedance changes observed in epilepsy for maximising the signal-to-noise ratio (SNR).

EIT studies of fast neural activity in the brain have used frequencies in the 1-2 kHz range to image physiological evoked activity or epileptic discharges with epicortical electrodes (Aristovich, et al., 2016; Vongerichten, et al., 2016). Although modelling indicated that the impedance change during neuronal depolarisation is maximal at DC and decreases with frequency, it is necessary to use a >1 kHz carrier frequency to avoid contamination of the impedance signal with: (a) resting-state EEG activity, and (b) artefacts due to the neural activity being measured (Oh, et al., 2011). With current applied at 1.7 kHz, the maximum fast impedance decrease occurring during averaged epileptic spikes in the cortex is c.0.3% (Vongerichten, et al., 2016; Hannan, et al., 2017). While this has enabled imaging of epileptic activity in cortical tissue, the magnitude of the impedance change measured from the cortical surface is known to be considerably smaller for neuronal activity originating in deep subcortical brain structures, such as the thalamus or hippocampus, due to dissipation of the signal (Faulkner, et al., 2017). Thus, optimising the carrier frequency for measuring fast neural activity during epilepsy is vital to increase SNR for imaging epileptic spikes originating below the cortex.

The longer-lasting slow impedance change during epileptic seizures has also been imaged in several EIT studies. An impedance increase of c.7 % was observed during localised seizures induced by electrical stimulation in the anaesthetised rabbit (Rao, 2000). EIT measurements were obtained using sixteen electrodes implanted on the cortical surface and a carrier frequency of 47 kHz (Rao, 2000). Fabrizi et al. attempted to image this signal with current injected through diametrically opposed scalp electrodes at 38.4 kHz in treatment-resistant epilepsy patients undergoing presurgical evaluation (Fabrizi, et al., 2006). However, no reproducible impedance changes with the expected duration of some tens of seconds and magnitude of 0.1 % from the scalp were observed, which was attributed to a low SNR due to hardware limitations (Fabrizi, et al., 2006). Preliminary imaging of slow impedance changes during chemically-induced cortical seizures in the anaesthetised rat revealed a maximal impedance increase of c.2.2 % (Vongerichten, et al., 2016). Since this study obtained measurements at 1.7 kHz, the frequency used for EIT of fast neural activity in the brain, it raises the question of whether a sufficient SNR may be achieved to image both the fast and slow changes during epileptic seizures at the same carrier frequency. This would enable measurement of the two impedance signals from a single seizure and is of clinical interest because seizures occur unpredictably, and often infrequently, during presurgical EEG-telemetry monitoring in patients with epilepsy. This issue has also been addressed by design of a parallel multi-frequency EIT system, in which current is injected simultaneously at different frequencies above 2 kHz, ideal for single-shot imaging of spontaneously occurring events like epileptic seizures (Dowrick, et al., 2015). An understanding of the frequency response of the fast and slow impedance changes will inform development of this system for imaging epileptic activity.

1.2. Purpose

The purpose of this work was to characterise the frequency response of two impedance signals associated with epileptic activity in the rat cerebral cortex: (a) the fast neural impedance change due to individual epileptic discharges, and (b) the slow impedance change occurring during seizures. Specific questions to be answered were:

(i) What are the characteristics of the fast and slow impedance signals during epileptiform activity across the comprehensive range of frequencies tested?
(ii) How do the fast and slow impedance responses compare to the known bioimpedance mechanisms occurring during hypersynchronous neuronal firing and cell swelling, respectively?
(iii) How do the findings compare to current understanding of the frequency responses of physiological signals from experimental data and biophysical modelling?
(iv) What are the implications for using EIT to image epileptic activity throughout the brain?

1.3. Experimental design

Impedance recordings were obtained using a 57-electrode epicortical array placed on the exposed surface of the cerebral cortex in the anaesthetised rat. Epileptiform events, which will henceforth be termed "seizures", were induced by electrically stimulating the sensorimotor cortex and comprised a pattern of highly repeatable ictal discharges. This epilepsy model was chosen as it enabled seizures to be induced on demand, allowing for total control of impedance measurements. Additionally, the electrographic features of ictal discharges within seizures and the seizures themselves remained stable over the course of experiments. As such, averaging of ictal discharges could be undertaken to enable characterisation of the fast neural impedance change, which is required due to its low magnitude. Furthermore, since seizures were electrographically reproducible, different carrier frequencies could be used to obtain impedance measurements from different seizures. Two electrodes within the epicortical array, located above the sensorimotor cortex, were electrically stimulated to induce seizures. During each seizure, impedance measurements were obtained by injecting current through another electrode pair at a given carrier frequency and recording voltages from all remaining electrodes on the array. Averaged impedance (dZ) values across rats are presented as absolute recorded voltages; these are directly representative of impedance because a constant amplitude current source was used to obtain measurements.

The frequency responses of fast and slow impedance changes were characterised using frequencies in the c.1-10 kHz range. Choosing a lower limit of 1 kHz ensured that noise from EEG activity could be drastically reduced and any artefacts due to ictal discharges could be eliminated from the impedance signal (Oh, et al., 2011). This was more relevant for the fast impedance change because a bandwidth of ±500 Hz around the carrier frequency was required to obtain a sufficient temporal resolution to characterise the response, whereas slow changes occurred over seconds and could be demodulated with a bandwidth as low as ±1 Hz. Both fast and slow signals were extracted from the same dataset to enable direct comparison of their responses across frequencies. Within the 1-10 kHz range, the lower frequencies (<3 kHz) were sampled with a finer spacing than those between 3 and 10 kHz. The frequencies were focused in this manner as it was expected that the optimal frequency for the fast impedance change may lie in this range, in accordance with the frequency response of somatosensory evoked activity in the cortex (Faulkner, et al., 2018). After analysis of the first dataset, this was confirmed to be an appropriate approach prior to conducting experimental repeats. At each frequency, impedance measurements were obtained using three different current injecting electrode pairs. Despite recording activity from all electrodes on the 57-electrode array, only the impedance measurements from the two recording electrodes that exhibited the largest impedance response were used to characterise responses.

2. Materials and methods

2.1. Animal preparation

Three adult female Sprague-Dawley rats (370-410 g) were used. Anaesthesia was induced with 4% isoflurane in 2 $Lmin^{-1}$ O_2 and an endotracheal intubation was performed to enable mechanical control of ventilation with 2-3% isoflurane in a 30/70 mixture of oxygen/air using an SAV03 small animal ventilator (Vetronic Services Ltd, Abbotskerswell, UK). The femoral artery and vein were cannulated, to allow for monitoring of intra-arterial blood pressure and intravenous access, respectively. Exhaled gases, respiratory rate, tidal volume, heart rate, invasive arterial blood pressure and SpO_2 were monitored regularly using an anaesthetic monitor (Lightning; Vetronic Services Ltd, Abbotskerswell, UK). Core body temperature was maintained at 36.5 ± 5 ^oC using a homeothermic heating unit comprising a blanket wrapped around the rat and a rectal thermistor probe providing feedback to the system (Harvard Apparatus, Edenbridge, UK). Rats were then fixed in a stereotaxic frame (Narishige International Ltd., London, UK), the skin of their head shaved and the scalp incised. The insertion of the temporal muscle on each side was cauterised using a bipolar coagulation unit (Codman Malis CMC-II; Codman, Raynham, MA) and incised with a scalpel. The cerebral cortex was exposed through a craniotomy in one hemisphere using a veterinary bone drill (Ideal Micro-Drill; Harvard Apparatus, Edenbridge, UK). The paramedial edge of the craniotomy extended from 1 mm anterior to lambda to 5 mm posterior to bregma, with the lateral boundary at the junction of the zygomatic to the temporal bone, forming a trapezoidal opening. The bone flap was lifted and the dura incised with micro scissors. Frequent irrigation of the area with 0.9 % sterile saline at 37 ^oC ensured the brain was kept moist. A 57-electrode planar array, fabricated from stainless steel foil and silicone rubber, was placed on the exposed cortical surface and a silver-silver chloride reference electrode, 9 mm in diameter, was placed beneath the nuchal skin. All voltage measurements were obtained with respect to this reference electrode. The 57-electrode array was trapezoidal in shape and measured 15 x 9 mm at its furthest edges, thus providing coverage of c.90 % of the cortical surface of one cerebral hemisphere. Electrodes were platinised prior to implantation to produce a contact impedance of ≤5 kΩ across the electrode-electrolyte interface. Following electrode implantation, anaesthesia was maintained with continuously-infused intravenous fentanyl at 20 µg/kg/hr (Eurovet Animal Health Ltd., Cambridge, UK) and c.0.5% isoflurane, reduced to the minimal concentration required to maintain surgical anaesthesia whilst ensuring maintenance of an areflexic state. All animal handling and experimental investigations undertaken in this study were ethically approved by the UK Home Office and performed in accordance with its regulations, as outlined in the Animals (Scientific Procedures) Act 1986.

2.2. Induction of seizures by cortical electrical stimulation

Seizures were induced by electrical stimulation of the sensorimotor cortex through two electrodes, with a centre-to-centre distance of 2.4 mm, on the 57-electrode epicortical array (**Fig. 1A,B**). Stimulation of the sensorimotor cortex was performed with a Keithley 6221 current source (Keithley Instruments Ltd, Bracknell, UK), controlled by custom MATLAB code. 5-s trains of biphasic, charge-balanced square-wave pulses with a pulse-width of 1 ms were delivered at a frequency of 100 Hz. 2 mA current was applied to produce a consistent electrocorticographic (ECoG) pattern of rhythmic ictal discharges. An inter-stimulus interval of 7 minutes prevented kindling of neural circuits over time to ensure that seizures remained consistent during recordings (Nelson, et al., 2010). Rats were paralysed prior to commencing EIT measurements with administered pancuronium bromide (1 mg/kg i.v.) to avoid introducing artefacts in the ECoG recordings due to motor manifestations of seizures. All procedures were performed on a vibration isolated table (Thorlabs Inc., Newton, NJ, USA).

2.3. EIT hardware and data acquisition

The ScouseTom EIT system comprises the BrainVision actiCHamp 128-channel EEG amplifier (Brain Vision LLC, Cary, NC) and Keithley 6221 current source (Keithley Instruments Ltd, Bracknell, UK (Avery, et al., 2017). The latter was used for current injection through an electrode pair on the 57-electrode epicortical array at a predefined carrier frequency and amplitude to obtain impedance measurements. The former was used for the simultaneous acquisition of ECoG and impedance recordings during each seizure. The epicortical array was fabricated using a 12.5 µm stainless steel foil sandwiched between two layers of silicone rubber. 57 electrode contacts, 0.6 mm in diameter and with a centre-to-centre distance of 1.2 mm, were exposed using a laser cutter and coated with platinum black in order to reduce contact impedance. Recordings were digitised at a sampling frequency of 50 kHz.

In each rat, three comprehensive frequency sweeps were performed to characterise the frequency response of impedance changes associated with both averaged ictal discharges and individual seizures. An individual frequency sweep comprised one single-channel impedance measurement at each of 20 different carrier frequencies of the injected current, one per seizure, ranging from 975 to 9975 Hz. For each impedance recording, a constant sinusoidal current was injected through a single pair of electrodes on the array at an amplitude of 50 µA. The impedance recording contained the seizure, in addition to baseline periods of ≥10 s prior to cortical stimulation and c.30 s after the end of the last ictal discharge. Current-injecting electrodes were positioned near the seizure focus, as determined by ECoG measurements, and the frequency addressing order was randomised in each sweep (**Fig. 1C**).

The BrainVision actiChamp EEG amplifier had a hardware anti-aliasing filter of 7.5 kHz. To account for any attenuation of the recorded signals due to this filter, its response was characterised across a resistor phantom in the frequency range of interest. The recorded impedance changes were then normalised by the inverse of this response, thus ensuring the observed responses were solely due to the induced epileptiform activity.

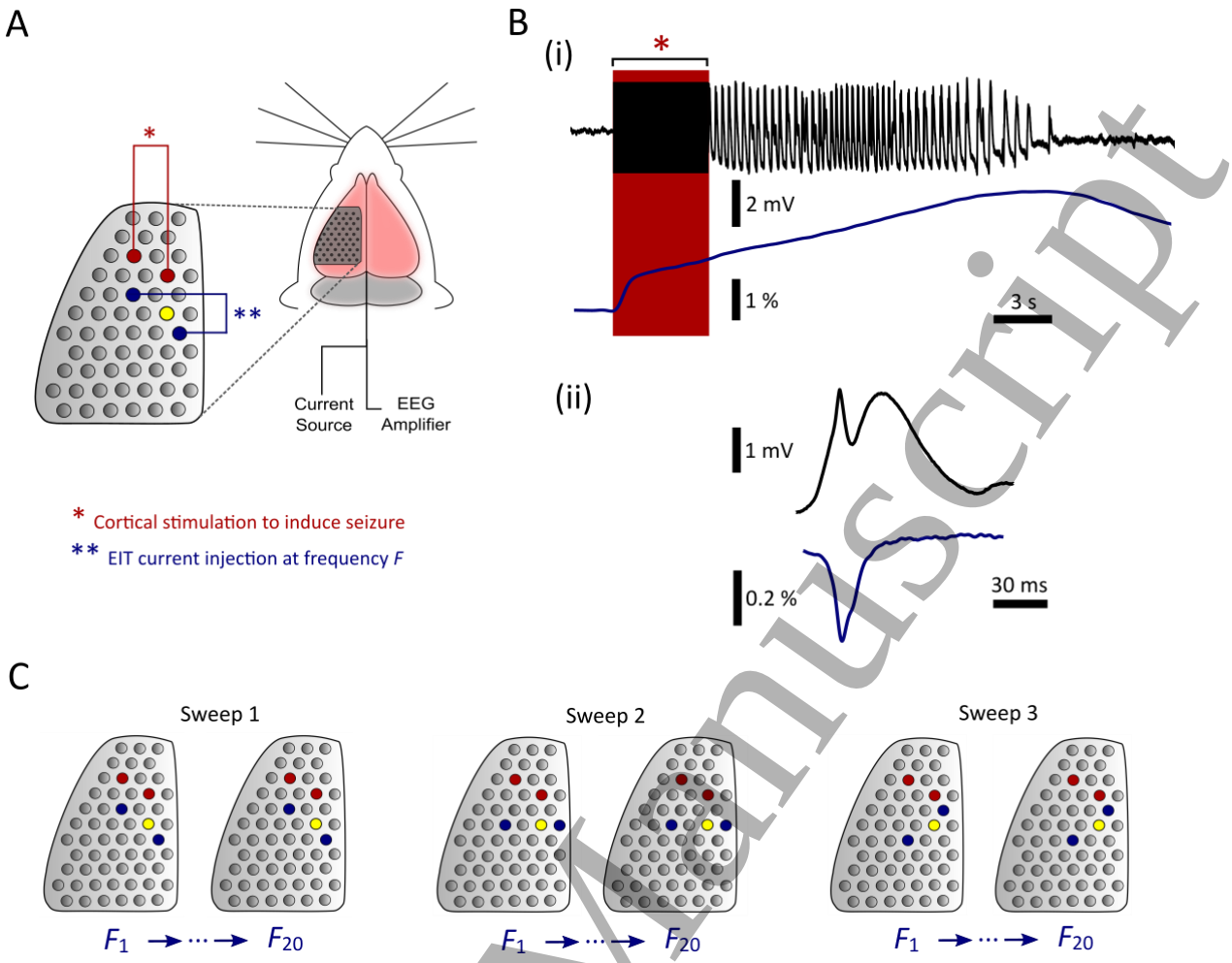

Figure 1. Schematic of experimental setup. (A) A 57-electrode epicortical array, connected to an EEG amplifier and two current sources, was placed on the exposed cortical surface of an anaesthetised rat. Two electrodes (red), which lay above the sensorimotor cortex, were stimulated with a 5-s train of 100 Hz biphasic square-wave pulses to induce seizures. Current was simultaneously injected through another electrode pair (blue), at a defined carrier frequency *F*, to obtain impedance measurements. The current-injecting electrode pairs were chosen around the seizure focus, defined as the electrode channel that displayed the highest-amplitude ictal discharges (yellow). **(B)** ECoG traces (black) of an entire seizure (i) and an averaged ictal discharge (ii) recorded from the electrode channel corresponding to the seizure focus. The associated slow (i) and fast (ii) impedance changes (blue) recorded from the same channel are shown beneath their respective ECoG events. **(C)** A single frequency sweep comprised current injection through the same electrode pair at 20 different carrier frequencies, ranging from 975 to 9975 Hz in a randomised order, one per seizure. Three sweeps, each with a different current injecting electrode pair, were undertaken in each subject.

2.4. Analysis of ECoG and impedance data

Single-injection impedance recordings at each carrier frequency were processed individually. The recorded raw voltage measurements contained both the ECoG and impedance signals; different filter settings were utilised to extract each of these. The ECoG signal was obtained by application of Butterworth filters at 1 kHz (low-pass, fifth order) and 1 Hz (high-pass, first order), in addition to a 50 Hz IIR notch filter (second order). To extract the fast impedance signal due to ictal discharges, the recording was filtered with a bandwidth of ±500 Hz around the carrier frequency (fifth-order Butterworth) and demodulated using the Hilbert transform. To extract the slow impedance signal during

an entire seizure, a bandwidth of ±1 Hz was used, which filtered out any artefacts due to cortical electrical stimulation.

Whereas the slow impedance response during individual seizures could be visualised in the demodulated impedance signal, the fast impedance response to individual ictal discharges was considerably smaller and so averaging was required to enable its characterisation (**Fig. 1B**). For this purpose, the ECoG channel displaying the highest-amplitude ictal discharges was selected as the trigger signal for subsequent spike detection and sorting. For each seizure, detection and classification of individual ictal spikes was performed using an automated spike classification algorithm in which the wavelet transform, which localises distinctive spike features, is combined with superparamagnetic clustering (Quiroga, et al., 2004). Ictal discharges were detected in the filtered ECoG data by setting an amplitude threshold of 1 mV from the baseline and defining the temporal window to be 120 ms before and after the peak amplitude; this enabled trigger markers to be set at the peak amplitude of all detected ictal spikes. The positions and classification of trigger markers for all epochs were verified by manual inspection and altered where necessary. The spike-and-wave discharge was the only type of ictal discharge that was seen consistently across all seizures in all rats; this was defined as the combination of a single sharp spike, <70 ms in duration and with a peak-peak amplitude of ± 2mV, followed by a slow wave component lasting c.100 ms. Only individual ictal discharges that lay within ±3 standard deviations (SDs) of the mean trace for all detected spikes in a given seizure were used for averaging. The demodulated impedance signals from all channels for each seizure were then aligned with respect to the trigger markers. For each electrode channel, the impedance change (dZ) associated with every ictal discharge was averaged within recordings, resulting in a mean dZ trace for ictal discharges within a seizure. A 150-ms temporal window around the trigger marker (30 ms before and 120 ms after), which encompassed the entire ictal discharge, was used for averaging.

For each single-channel impedance recording, impedance measurements from the two electrodes that exhibited the largest impedance changes during both the averaged ictal discharge and seizure were chosen for further analysis to characterise their respective frequency responses. Thus, two impedance measurements were obtained for each of the three frequency sweeps per animal, and data was collected in three animals, resulting in a total of 18 impedance traces at each frequency for both ictal spikes and seizures.

The frequency responses for ictal discharges and seizures were characterised by determining the maximum amplitude of the impedance signal and SNR for each channel used. SNR was computed by dividing the maximum amplitude of the impedance signal by the SD of the corresponding baseline. For ictal discharges, the baseline period was defined as the first 10 ms of the 150-ms temporal window used for averaging. For seizures, a 5-s epoch immediately prior to cortical stimulation was used as the baseline and seizure duration was defined as the time period between the appearance of the first and last ictal spike. The slow impedance change typically consisted of a steady increase in impedance which began during the cortical stimulation period and peaked near the end of the seizure (**Fig. 1B(i)**). Due to the limited length of impedance recordings, to minimise damage caused by continuous current delivery to cortical tissue, it was not possible in some seizures to see the slow impedance change completely return to baseline. However, in all cases, a clear peak in impedance was observed. The maximum impedance change and SNR values at each frequency were determined from the 18 impedance traces and averaged together.

2.5. Statistical analysis

It was important to ensure that the electrographic presentation of these epileptiform events remained stable during each frequency sweep and was not affected by the carrier frequency used for impedance recordings. One-way analysis of variance (ANOVA) tests were conducted to confirm that there was no significant difference in the maximal ECoG amplitude of averaged ictal discharges or the seizure duration, defined as the time period between the appearance of the first and last ictal discharge in the ECoG, across frequencies.

Our null hypothesis was that there is no difference in the SNR of impedance changes recorded across carrier frequency; we were therefore testing for frequencies at which the SNR was statistically significant in individual animals and showing the reproducibility of the result. Since the differences in physiological conditions within the same animal were being evaluated, measurements obtained in each of the three animals could be considered statistically independent. ANOVA tests were conducted to determine whether there were statistically significant differences in SNR for fast and slow impedance changes across frequency. To identify the frequencies at which any statistical significances lay, the SNR at each frequency was compared to the mean SNR across all 20 frequencies using a one-tailed t-test. A significance level of $\alpha = 0.01$ was used for all statistical analyses and all data are presented as mean ± SD.

3. Results

3.1. Reproducibility of electrically-induced epileptiform events

To avoid introducing anomalies into the results, all rats were tested prior to experimentation to ensure that the expected electrographic patterns of epileptiform events were observed. Indeed, seizures comprising a characteristic pattern of repeatable ictal discharges, which consisted of 5 Hz ictal spike-and-wave discharges which subsequently slowed to 2-3 Hz sharp waves, were reliably induced by electrical stimulation with 2 mA biphasic square-wave pulses in all animals. The requisite first step in assessing the frequency response of impedance changes associated with ictal discharges (fast changes) and seizures (slow changes) was to confirm that these events stayed consistent over time and were not affected by the frequency of current applied to obtain the impedance measurement. Ictal discharges exhibited a high degree of electrographic reproducibility within and across rats; this was evidenced by low variance in the waveform shape, duration and inter-spike interval. The peak ECoG amplitude of averaged ictal spikes, recorded from the channel on the 57-electrode array with the largest response for each seizure, had a mean of 2.14 mV ± 0.96 mV across rats and was not significantly different across the range of carrier frequencies tested ($p > 0.01$, $n = 180$). Mean seizure duration was 16.7 ± 6.8 ms and was also not affected by frequency ($p > 0.01$, $n = 180$). Randomisation of the frequency addressing order in every sweep further validated any observed effects of frequency on the measured impedance change. Furthermore, the maximal ECoG and impedance signals were consistently recorded from the same electrodes located above the seizure focus, 3 mm posterior to the sensorimotor cortex. Due to this high repeatability in seizure presentation, functional variability across animals was deemed to be sufficiently low.

3.2. Frequency response of fast impedance change during ictal discharges

For the fast impedance change due to neuronal activity during ictal discharges, the peak impedance change (dZ) observed at a carrier frequency of 975 Hz was -19.4 ± 5.9 µV (-0.22 ± 0.06 %) (**Fig. 2A**). dZ increased with frequency until 1355 Hz, at which point a maximum dZ value of -41.1 ± 9.2 µV (-0.36 ± 0.05 %) was achieved. Between 1355 and 2975 Hz, the dZ decreased to -3.1 ± 0.7 µV (-0.05 ± 0.03 %) and remained relatively stable at frequencies above 2975 Hz.

The SNR of this response followed a similar trend. It increased from 16.2 ± 5.6 at 975 Hz to a maximal value of 50.2 ± 11.3 at 1355 Hz, before decreasing to a minimum of 3.5 ± 0.9 at 3475 Hz (**Fig. 2B**). The SNR achieved at frequencies ranging from 1225 to 1605 Hz was significantly higher than the mean SNR across all frequencies ($p < 0.01$, n = 18 impedance measurements, N = 3 rats; $p = 2.37 \times 10^{-13}$ at 1355 Hz).

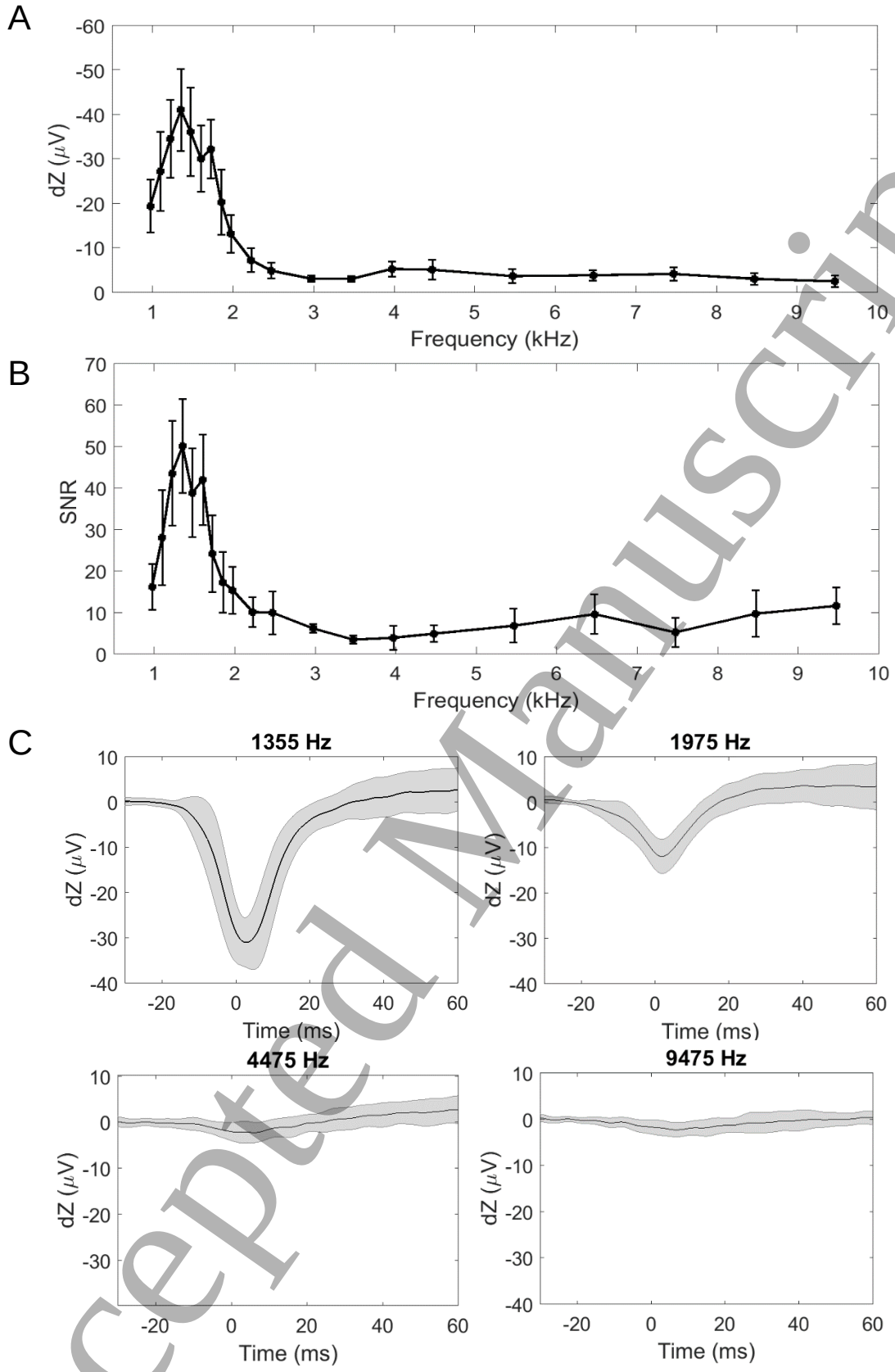

Figure 2. Frequency response of fast impedance change during ictal discharge. (A) Peak impedance change (dZ) during ictal discharges recorded from the cortical surface with varying carrier frequency. **(B)** SNR of the fast impedance signal with varying carrier frequency. **(C)** Examples of impedance traces obtained with four carrier frequencies: 1355 Hz, 1975 Hz, 4475 Hz and 9475 Hz. Time is given with respect to the peak amplitude of the ictal discharge in the ECoG recording. All dZ and SNR values are given as mean ± SD.

3.3. Frequency response of slow impedance change during seizures

The slow impedance change due to cell swelling during seizures had a peak amplitude of 3.13 ± 0.26 mV (4.82 ± 1.52 %) at a frequency of 975 Hz (**Fig. 3A**). The magnitude of the peak impedance change decreased with increasing frequency, reaching a minimum value of 0.76 ± 0.16 mV (1.44 ± 1.17 %) at 9475 Hz, the highest carrier frequency tested.

The SNR for the slow dZ increased from 452 ± 67 at 975 Hz to a maximal value of 614 ± 112 at 1975 Hz. It then decreased with frequency to a minimum of 89 ± 18 at 9475 Hz (**Fig. 3B**). However, no significant differences in the SNR was observed across the range of frequencies tested ($p > 0.01$, $n = 18$ impedance measurements, $N = 3$ rats).

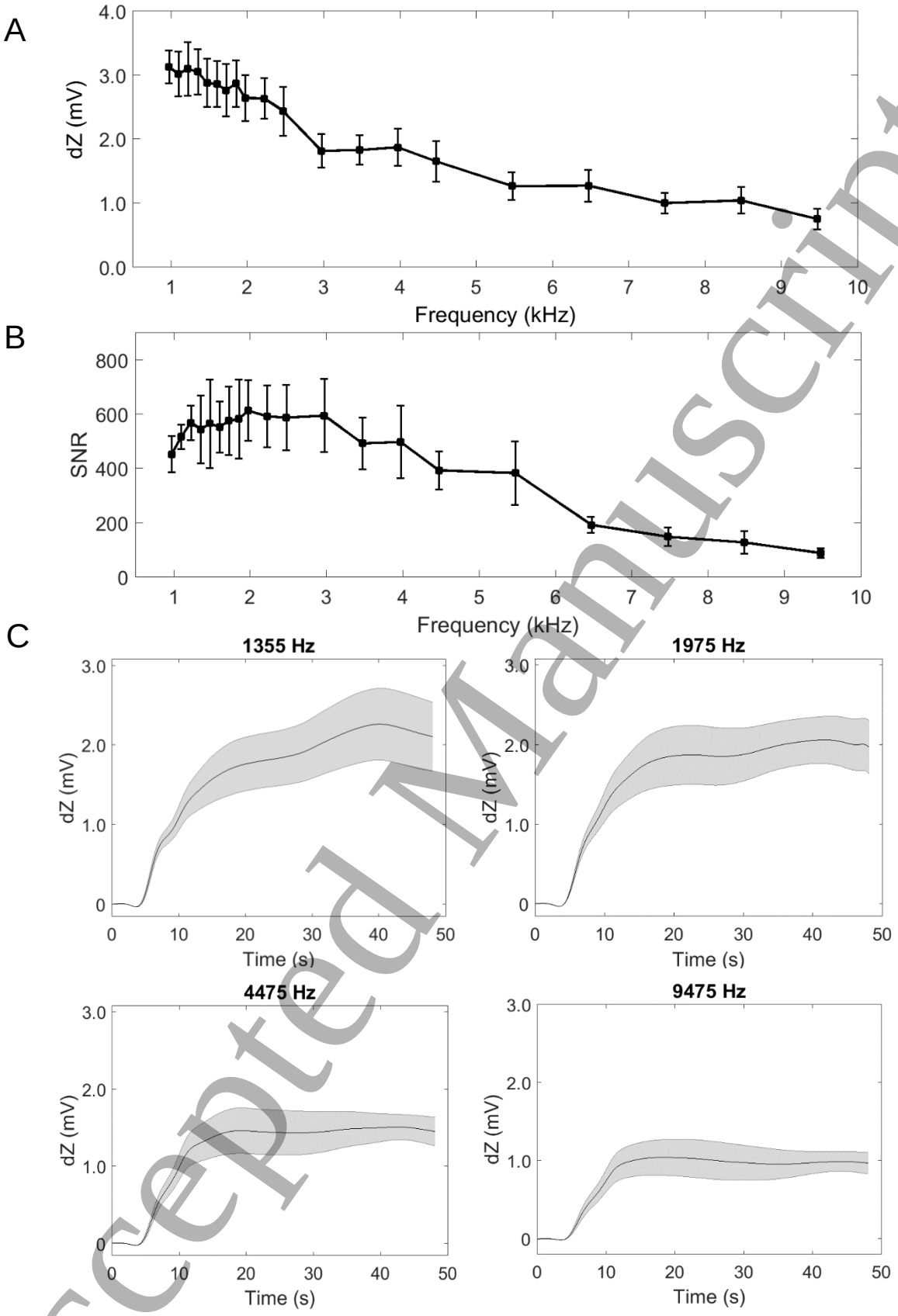

Figure 3. Frequency response of slow impedance change during seizures. (A) Peak impedance change (dZ) during slow changes recorded from the cortical surface with varying carrier frequency. **(B)** SNR of the slow impedance signal with varying carrier frequency. **(C)** Examples of impedance traces obtained with four carrier frequencies: 1355 Hz, 1975 Hz, 4475 Hz and 9475 Hz. Electrical stimulation of the cortex to induce seizures occurred at 4-9 s. All dZ values are given as mean ± SD.

4. Discussion

4.1. Summary of results

The same trend in amplitude and SNR of impedance changes with frequency were observed within and across animals. The magnitude and SNR of the fast neural impedance change associated with ictal discharges were both largest at 1355 Hz and gradually decreased at frequencies above this. For the slow impedance change which occurred due to cell swelling during the seizure, the maximum signal and SNR were observed at 975 Hz and 1975 Hz, respectively. Although the magnitude of the impedance change and SNR both continued to decrease with increasing frequency, the SNR was not significantly different across carrier frequencies.

4.2. Characteristics of fast and slow impedance changes during epileptiform activity across frequency

During ictal discharges, a fast, transient decrease in cortical tissue impedance was observed which can be attributed to hypersynchronous depolarisation of local neuron populations. The longer-lasting impedance change which occurred due to cell swelling during the seizure, on the other hand, was positive and typically two orders of magnitude larger than that recorded during averaged ictal discharges at any of the carrier frequencies tested.

For the fast impedance change, the maximum signal and SNR were observed at a carrier frequency of 1355 Hz (**Fig. 2**). The impedance change and SNR both increased between 975 Hz to 1355 Hz, and then proceeded to decrease with frequency until 2975 Hz. Although the magnitude of the impedance signal plateaued at this point and remained relatively constant at frequencies >3 kHz, the SNR increased between 3 and 10 kHz from 3.5 ± 0.9 to 11.7 ± 4.4. This increase in SNR may be attributed to reduced noise when injecting current at higher frequencies.

The frequency response observed for the slow impedance change during seizures differed to that of the fast change in several respects. First, the maximal impedance change was observed at a 975 Hz and displayed a monotonic decrease with frequency until 9475 Hz, the highest frequency tested, rather than reaching a plateau (**Fig. 3A**). Secondly, the SNR displayed a similar general trend across frequency to this maximal impedance signal and, unlike the fast changes, did not increase above 3 kHz (**Fig. 3B**). This is due to the fact that a bandwidth of 1 Hz round the carrier frequency was used for demodulation of these slow impedance changes. Thus, the effect of decreased noise at frequencies >3 kHz was negligible, in contrast to the fast impedance changes, for which it was necessary to use a 500 Hz bandwidth to obtain the required temporal resolution of 2 ms. Lastly, the changes in SNR across frequency were not statistically significant and so did not point to a single optimal frequency within the range tested for imaging slow impedance changes in the cortex.

4.3. Comparison of findings to current understanding of bioimpedance mechanisms of epilepsy and frequency responses of such physiological signals

4.3.1. Fast impedance changes

Previous EIT studies aimed at imaging neural activity in the cortex during epilepsy used a frequency of 1.7 kHz frequency and reported a maximum impedance change of c.-0.3% for both interictal and ictal epileptiform discharges, in chemical and electrical models of epilepsy in the anaesthetised rat, respectively (Vongerichten, et al., 2016; Hannan, et al., 2017). The fast impedance change which occurred at 1.7 kHz during the spiking component of averaged ictal discharges in the current study was consistent with these findings. However, this value reached its peak of c.0.4 % when using a carrier frequency of 1355 Hz, suggesting that this is the optimal frequency for recording fast neural impedance changes during epileptiform discharges in cortical tissue.

The observed trends in amplitude and SNR of the fast impedance change differed from the monotonic decrease in impedance with frequency from DC predicted by biophysical models of neural activity (Liston, et al., 2012; Tarotin, et al., 2017). This may be explained by limitations of these modelling studies which include the fact that the former is based only on the passive properties of neuronal membranes (Liston, et al., 2012) and the latter only considered interactions between unmyelinated nerve fibres in the peripheral nervous system (Tarotin, et al., 2017). Since physiological or pathological activity in neural networks of the brain typically involve complex interactions between unmyelinated and myelinated axons, driven by active voltage- and ligand- gated ionic conductances, it is unsurprising that these models were unable to predict the frequency response observed during epileptiform activity.

Our findings are more comparable, however, to the frequency response of impedance changes recorded during somatosensory evoked potentials in the rat cortex and thalamus (Faulkner, et al., 2018). During this physiological activity, a significant SNR was obtained in the cortex at 1325-2225 Hz and the largest magnitude of the impedance change and SNR were observed at 1475 Hz in both brain structures (Faulkner, et al., 2018). Thus, the non-monotonic frequency response of fast neural activity observed in the present study, in which significant frequencies for recording cortical impedance changes lay in the 1225-1605 Hz range, are highly similar to those obtained previously. This was expected as the same cortical pyramidal neurons and thalamocortical neural circuits are thought to be involved in generating both somatosensory evoked potentials and epileptiform discharges originating in the cortex (Blumenfeld, 2005). However, it is interesting that the peak impedance response and SNR were obtained at 1355 Hz in the present study and 1475 Hz for the physiological activity characterised previously (Faulkner, et al., 2018). To generate epileptiform discharges in the cortex, a higher proportion of cortical neurons must generally be recruited to fire in synchrony compared to somatosensory evoked potentials (Elur, 1967; Stafstrom, 2005; Murakami & Okada, 2006); this is evident in the EEG as a sharper and higher-amplitude burst of activity, which in turn manifests in a larger tissue impedance change. Since different patterns of neuronal activity are known to have differing intrinsic frequency preferences for resonance (Hutcheon & Yarom, 2000), this may explain the slight difference observed in optimal carrier frequency between physiological and epileptiform activity.

4.3.2. Slow impedance changes

Several studies have demonstrated an increase in cerebral tissue impedance due to cell swelling during seizures using current injected within the 1-10 kHz range of frequencies tested. Van Harreveld & Schadé (1962) and Elazar, et al. (1966) measured impedance changes of c.3.5-5 % at 1 kHz from cortical surface and hippocampal depth electrodes, respectively, in electrical and chemical models of epilepsy in rabbits and cats. This is consistent with the c.4.8 % impedance increase recorded from the rat cortex at 975 Hz in the present work. Using current injected at 1.7 kHz, Vongerichten et al. (2016) reported a cortical impedance change of c.2.2 % during chemically-induced seizures in the anaesthetised rat. This differs from the c.4.1 % change observed here at the same frequency, which may be attributed to the different epilepsy model used. In contrast to chemical convulsant agents, the cortical electrical stimulation model used here lacks cell-type specificity (Kandratavicius, et al., 2014). Thus, it is possible that a a greater number of cortical principal cells were activated during seizures in the current work, leading to the greater impedance change.

In contrast to the fast neural response, which is controlled by an active system, the frequency response of the slow impedance change is the result of a passive system. Thus, the overall monotonic decrease in impedance with frequency was expected based on prior modelling and may be explained by the capacitive transfer of current across cell membranes. During cell swelling, the volume of the extracellular fluid is decreased. As the majority of current applied in the 1-10 kHz frequency range is conducted through the extracellular fluid, this causes an impedance increase (Seoane, et al., 2005). However, a small amount of current is transferred capacitively into the intracellular space. This amount increases as the carrier frequency of applied current is increased due to the more rapidly reversing flux

of charge across the capacitance of the neuronal cell membrane (Holder, 2005b). As a result, the magnitude of the measured impedance change is lower at higher frequencies.

The SNR of the seizure-induced slow impedance change did not change significantly across frequency, showing that an adequate SNR for imaging this signal can be achieved with any frequency lying in the 1-10 kHz range. Previous modelling and *in vivo* experiments aimed at testing the effects of frequency on the impedance change caused by pathological cell swelling utilised higher frequencies ranging from 20 to 750 kHz (Seoane, et al., 2005). Thus, the present study provides, for the first time, a characterisation of the frequency response of this slow impedance change at frequencies that may simultaneously be used to measure fast neural activity during epileptiform discharges.

4.4. Implications for EIT imaging of epileptic activity

We have characterised the frequency response of two impedance signals, fast and slow, associated with epileptic activity in the rat cerebral cortex. Our findings indicate an optimal carrier frequency of 1355 Hz for measuring the fast impedance change occurring due to hypersynchronous neuronal depolarisation during an individual ictal epileptiform discharge. Because EIT is known to have a somewhat limited depth penetration, it is of paramount importance to maximise SNR to image brain activity in regions deeper than the cortex. Therefore, we conclude that using a frequency of 1355 Hz will provide the best chance of imaging fast neural activity of epileptiform discharges originating in subcortical brain structures, such as the hippocampus or thalamus, from the cortical surface.

In contrast to the fast change, the longer-lasting slow impedance change occurring over the course of the seizure, due to cell swelling secondary to the hypersynchronous neuronal firing, had a sufficiently high SNR at all frequencies tested in the 1-10 kHz range. Thus, for future studies aiming to image epileptiform activity with EIT, we recommend using a carrier frequency of 1355 Hz which would enable localisation of both the fast and slow impedance changes, consequently maximising the spatiotemporal information obtained from a single ictal event. This would be particularly important for telemetry monitoring of epileptic activity in a clinical setting since seizures often occur infrequently. The ability to correlate the measured impedance changes to ictal semiology would also have broad implications in critical care. Alterations in impedance may be used to distinguish between ictal and indeterminate rhythms in cases of electroclinical dissociation, for example, a characteristic feature of neonatal seizures (Weiner, et al., 1991). Additionally, the ability to image the neural activity and slower metabolic changes simultaneously with EIT holds potential to aid elucidation of the mechanisms of seizure initiation and expression.

Parallel multi-frequency EIT, which involves simultaneous current injection at different carrier frequencies, is an appealing method for imaging short-duration, spontaneous epileptic events (Dowrick, et al., 2015). For such applications, the recommendation from the present work is to use frequencies between 3 and 10 kHz, as this is the range at which the magnitude and shape of the fast neural impedance change remained relatively constant. Additionally, a separation of at least 500 Hz between all chosen frequencies should be used as this is the required bandwidth around the carrier frequency to obtain an adequate temporal resolution for imaging fast neural activity. These settings would also allow for simultaneously measuring the slow impedance change which had a sufficiently high SNR at all frequencies.

Acknowledgements

This work was supported by DARPA (N66001-16-2-4066), Blackrock Microsystems and the EPSRC (EP/M506448/1).

References

Andrew, R. D. (1991). Seizure and acute osmotic change: clinical and neurophysiological aspects. *J Neurol Sci, 101*(1), 7-18.

Andrew, R. D., & MacVicar, B. A. (1994). Imaging cell volume changes and neuronal excitation in the hippocampal slice. *Neuroscience, 62*(2), 371-383.

Aristovich, K. Y., Packham , B. C., Koo, H., dos Santos, G. S., McEvoy, A., & Holder, D. S. (2016). Imaging fast electrical activity in the brain with electrical impedance tomography. *Neuroimage, 124*(Pt A), 204-213.

Avanzini, G., Panzica, F., & de Curtis, M. (2000). The role of the thalamus in vigilance and epileptogenic mechanisms. *Clin Neurophysiol, 111*(Suppl 2), 19-26.

Avery, J., Dowrick, T., Faulkner, M., Goren, N., & Holder, D. S. (2017). A Versatile and Reproducible Multi-Frequency Electrical Impedance Tomography System. *Sensors (Basel), 17*(2), E280.

Binder, D. K., & Haut, S. R. (2013). Toward new paradigms of seizure detection. *Epilepsy Behav, 26*(3), 247-252.

Blumenfeld, H. (2005). Cellular and network mechanisms of spike-wave seizures. *Epilepsia, 46*(9), 21-33.

Boone, K., Lewis, A. M., & Holder, D. S. (1994). Imaging of cortical spreading depression by EIT: implications for localization of epileptic foci. *Physiol Meas, 15*(Suppl 2a), A189-198.

Broberg, M., Pope, K. J., Lewis, T., Olsson, T., Nilsson, M., & Willoughby, J. O. (2008). Cell swelling precedes seizures induced by inhibition of astrocytic metabolism. *Epilepsy Res, 80*(2-3), 132-141.

Buzsáki, G. (1991). The thalamic clock: emergent network properties. *Neuroscience, 41*(2-3), 351-364.

Cain, S. M., & Snutch, T. P. (2012). Chapter 6: Voltage-gated calcium channels in epilepsy. In J. L. Noebels et al. (Ed.), *Jasper's basic mechanisms of the epilepsies.* Oxford: Oxford University Press.

Cain, S. M., & Snutch, T. P. (2012). Chapter 6: Voltage-gated calcium channels in epilepsy. In J. L. Noebels, M. Avoli, & M. A. Rogawski (Eds.), *Jasper's basic mechanisms of the epilepsies.* Oxford: Oxford University Press.

Cole, K. S. (1928). Electrical impedance of suspensions of spheres. *J Gen Physiol, 12*(1), 29-36.

Dowrick, T., Sato dos Santos, G., Vongerichten, A., & Holder, D. (2015). Parallel, multi frequency EIT measurement, suitable for recording impedance. *J Electr Biomp, 6*, 37-43.

Dreier, J. P., Major, S., Pannek, H. W., Woitzik, J., Scheel, M., Wiesenthal, D., Martus, P., Winklet, M.K., Hartings, J., Fabricius, M., Speckmann, E. J., & Gorji, A. (2011). Spreading convulsions, spreading depolarization and epileptogenesis in human cerebral cortex. *Brain, 135*(Pt 1), 259-275.

Dzhala, V., Ben-Ari, Y., & Khazipov, R. (2000). Seizures accelerate anoxia-induced neuronal death in the neonatal rat hippocampus. *Ann Neurol, 48*(4), 632-640.

Elazar, Z., Kado, R. T., & Adey, W. R. (1966). Impedance changes during epileptic seizures. *Epilepsia, 7*(4), 291-307.

Elur, R. (1967). Amplitude histograms of the EEG as an indicator of the cooperative behavior of neuron populations. *Electroencephalogr Clin Neurophysiol, 23*(1), 87.

Fabrizi, L., Sparkes, M., Horesh, L., Perez-Juste Abascal, J. F., McEwan, A., Bayford, R. H., Elwes, R., Binnie, C. D., & Holder, D. S. (2006). Factors limiting the application of electrical impedance tomography for identification of regional conductivity changes using scalp electrodes during epileptic seizures in humans. *Physiol Meas, 27*(5), S163-174.

Faulkner, M., Hannan, S., Aristovich, J., Avery, J., & Holder, D. (2018). Characterising the frequency response of impedance changes during. *Physiol Meas,39*(3), 034007.

Faulkner, M., Hannan, S., Aristovich, K., & Holder, D. (2017). Recording thalamic impedance changes to assess feasability of 3D EIT. Hanover, NH, USA: 18th Int Conf on Biomedical Applications of Electrical Impedance Tomography.

Hannan, S., Faulkner, M., Aristovich, K., Avery, J., & Holder, D. S. (2017). Imaging epileptic activity in the rat brain with three-dimensional electrical impedance tomography. Dartmouth College, USA: 18th Int Conf on Biomedical Applications of Electrical Impedance Tomography.

Hodgkin, A. L., & Huxley, A. F. (1952). A quantitative description of membrane current and its application to conduction and excitation in nerve. *J Physiol, 117*(4), 500-544.

Holder, D. S. (2005a). *Electrical Impedance Tomography: methods, history and application.* Bristol: Institute of Physics Publishing.

Holder, D. S. (2005b). Appendix A: Brief introduction to bioimpedance. In D. S. Holder (Ed.), *Electrical Impedance Tomography: methods, history and applications* (pp. 411-422). Bristol: Institute of Physics Publishing.

Hutcheon, B., & Yarom, Y. (2000). Resonance, oscillation and the intrinsic frequency preferences of neurons. *Trends Neurosci, 23*(5), 216-222.

Jefferys, J. G. (1995). Nonsynaptic modulation of neuronal activity in the brain: electric currents and extracellular ions. *Physiol Rev, 75*(4), 689-723.

Kandratavicius, L., Balista, P. A., Lopes-Aguiar, C., Ruggiero, R. N., Umeoka, E. H., Garcia-Cairasco, N., Bueno-Junior, L. S., & Leite, J. P. (2014). Animal models of epilepsy: use and limitations. *Neuropsychiatr Dis Treat, 10*, 1693-1705.

Klivington, K. A., & Galambos, R. (1967). Resistance shifts accompanying the evoked cortical response in the cat. *Science, 157*(3785), 211-213.

Liston, A., Bayford, R., & Holder, D. (2012). A cable theory based biophysical model of resistance change in crab peripheral nerve and human cerebral cortex during neuronal depolarisation: implications for electrical impedance tomography of fast neural activity in the brain. *Med Biol Eng Comput, 50*(5), 425-437.

Murakami, S., & Okada, Y. (2006). Contributions of principal neocortical neurons to magnetoencephalography and electroencephalography signals. *J Physiol, 575*(Pt 3), 925-936.

Nelson, T. S., Suhr, C. L., Lai, A., Halliday, A. J., Freestone, D. R., McLean, K. J., Burkitt, A. N., & Cook, M. J. (2010). Seizure severity and duration in the cortical stimulation model of experimental epilepsy in rats: a longitudinal study. *Epilepsy Res, 89*(2-3), 261-270.

Oh, T., Gilad, O., Ghosh, A., Schuettler, M., & Holder, D. S. (2011). A novel method for recording neuronal depolarization with recording at 125-825 Hz: implications for imaging fast neural activity in the brain with electrical impedance tomography. *Med Biol Eng Comput, 49*(5), 593-604.

Olsson, T., Broberg, M., Pope, K. J., Wallace, A., Mackenzie, L., Blomstrand, F., Nilsson, M., & Willoughby, J. O. (2006). Cell swelling, seizures and spreading depression: an impedance study. *Neuroscience, 140*(2), 505-515.

Quiroga, R. Q., Nadasdy, Z., & Ben-Shaul, Y. (2004). Unsupervised spike detection and sorting with wavelets and superparamagnetic clustering. *Neural Commut, 16*(8), 1661-1687.

Rao, A. (2000). Electrical impedance tomography of brain activity: studies into its accuracy and physiological mechanisms. *PhD thesis, University College London, UK*.

Seoane, F., Lindecrantz, K., Olsson, T., Kjellmer, I., Flisberg, A., & Bågenholm, R. (2005). Spectroscopy study of the dynamics of the transencephalic electrical impedance in the perinatal brain during hypoxia. *Physiol Meas, 26*(5), 849-863.

Stafstrom, C. E. (2005). Neurons Do the Wave (and the Spike!) during Neocortical Seizures. *Epilepsy Curr, 5*(2), 69-71.

Stafstrom, C. E. (2007). Persistent sodium current and its role in epilepsy. *Epilepsy Curr, 7*(1), 15-22.

Tarotin, I., Aristovich, K., & Holder, D. (2017). Model of impedance change in unmyelinated fibres. Hanover, NH, USA: 18th Int Conf on Biomedical Applications of Electrical Impedance Tomography.

Van Harreveld, A., & Schadé, J. P. (1962). Changes in the electrical conductivity of cerebral cortex during seizure activity. *Exp Neurol, 5*, 383-400.

Velluti, R., Klivington, K., & Galambos, R. (1968). Evoked resistance shifts in subcortical nuclei. *Curr Mod Biol, 2*(2), 78-80.

Vongerichten, A. N., dos Santos, G. S., Aristovich, K., Avery, J., McEvoy, A., Walker, M., & Holder, D. S. (2016). Characterisation and imaging of cortical impedance changes during interictal and ictal activity in the anaesthetised rat. *Neuroimage, 124*(Pt A), 813-823.

Weiner, S. P., Painter, M. J., Geva, D., Guthrie, R. D., & Scher, M. S. (1991). Neonatal Seizures: Electroclinical dissociation. Pediatric Neurol, 7, pp. 363-368.